

Enhanced output performance of flexible piezoelectric energy harvester by using auxetic graphene films as electrodes

Cite as: Appl. Phys. Lett. **117**, 103901 (2020); <https://doi.org/10.1063/5.0015100>

Submitted: 24 May 2020 . Accepted: 28 August 2020 . Published Online: 10 September 2020

Huazhang Zhang, Pin Wen, Peng Li, Zhe Wang, Suyan Wang, Xin Zhao, Yong Xiao, Jie Shen, Daping He , and Wen Chen

COLLECTIONS

 This paper was selected as an Editor's Pick



View Online



Export Citation



CrossMark

ARTICLES YOU MAY BE INTERESTED IN

[Experimental determination of the {111}/{001} surface energy ratio for Pd crystals](#)

Applied Physics Letters **117**, 101601 (2020); <https://doi.org/10.1063/5.0022879>

[Visible-to-near-infrared organic photodiodes with performance comparable to commercial silicon-based detectors](#)

Applied Physics Letters **117**, 093302 (2020); <https://doi.org/10.1063/5.0018274>

[Direct epitaxial nanometer-thin InN of high structural quality on 4H-SiC by atomic layer deposition](#)

Applied Physics Letters **117**, 093101 (2020); <https://doi.org/10.1063/5.0014900>



Your Qubits. Measured.

Meet the next generation of quantum analyzers

- Readout for up to 64 qubits
- Operation at up to 8.5 GHz, mixer-calibration-free
- Signal optimization with minimal latency

Find out more

 Zurich Instruments

Enhanced output performance of flexible piezoelectric energy harvester by using auxetic graphene films as electrodes

Cite as: Appl. Phys. Lett. **117**, 103901 (2020); doi: [10.1063/5.0015100](https://doi.org/10.1063/5.0015100)

Submitted: 24 May 2020 · Accepted: 28 August 2020 ·

Published Online: 10 September 2020




View Online



Export Citation



CrossMark

Huazhang Zhang,^{1,2} Pin Wen,³ Peng Li,¹ Zhe Wang,¹ Suyan Wang,² Xin Zhao,¹ Yong Xiao,² Jie Shen,² Daping He,^{1,2,a)}  and Wen Chen^{2,a)}

AFFILIATIONS

¹Hubei Engineering Research Center of RF-Microwave Technology and Application, School of Science, Wuhan University of Technology, Wuhan 430070, China

²State Key Laboratory of Advanced Technology for Materials Synthesis and Processing, School of Materials Science and Engineering, Wuhan University of Technology, Wuhan 430070, People's Republic of China

³Hubei Key Laboratory of Theory and Application of Advanced Materials Mechanics, School of Science, Wuhan University of Technology, Wuhan 430070, China

^{a)}Authors to whom correspondence should be addressed: hedaping@whut.edu.cn and chenw@whut.edu.cn

ABSTRACT

We demonstrate an effective approach to enhance the output performance of a flexible piezoelectric energy harvester by using flexible electrodes with negative Poisson's ratio (NPR). The relationship between open-circuit voltage and Poisson's ratio of electrodes is established theoretically by deriving the analytical expression. It reveals a continuous increasing trend in open-circuit voltage with the decrease in Poisson's ratio of the electrodes. Further, graphene-assembled macro-film (GAMF), an NPR material with excellent flexibility and high conductivity, is used as the electrodes to fabricate flexible piezoelectric energy harvesters. Compared with the energy harvesters using silver electrode, the harvesters made by GAMF electrodes, with an NPR of -0.39 , achieve nearly 1.7-times enhancement in open-circuit voltage and 1.6-times in short-circuit current for output performance. The experimental results are highly consistent with the simulation results, indicating that the GAMF has great prospects in developing flexible piezoelectric energy harvesters with enhanced electrical output performance.

Published under license by AIP Publishing. <https://doi.org/10.1063/5.0015100>

Flexible piezoelectric energy harvesting, which converts the ambient mechanical energy into useful electricity through piezoelectric transduction, has the potential to provide facile and environmental-friendly power supply for usage in portable and wearable electronics.^{1–5} Compared with other ambient energy harvesting techniques, the flexible piezoelectric energy harvesting method has many advantages, such as direct conversion, high efficiency, wearing comfort, easy miniaturization and integration, independence of time and location, etc.^{6–8} However, the electricity generated by most of the currently reported flexible piezoelectric energy harvesters is insufficient for practical uses. Hence, research efforts toward improving the output performance of flexible piezoelectric energy harvesters are necessary.^{9–13}

Extensive research has been carried out to promote the output performance of flexible piezoelectric energy harvesters, and most of

them are focused on the optimization of piezoelectric materials.¹⁴ Various kinds of piezoelectric materials, including nanomaterials,^{15–18} polymers,^{19–21} inorganic films,^{22–27} and organic–inorganic composites,^{28–31} with excellent flexibility and piezoelectricity have been developed. Besides the optimization of piezoelectric materials, the optimization of the mechanical structure of the flexible piezoelectric energy harvesting devices could also be an effective approach for improving the output performance. By incorporating appropriate mechanical design, the applied stress or strain can be amplified and concentrated onto the piezoelectric material, and the working mode can also be intentionally selected and hybridized so as to improve the performance of the piezoelectric energy harvester. The strategies of mechanical structure optimization have been extensively used in piezoelectric vibration energy harvesters and proved to be effective.^{32,33} To work in resonance vibration mode, a certain stiffness of the devices

is required and, therefore, these piezoelectric vibration energy harvesters usually display poor flexibility. For the flexible piezoelectric energy harvesters, which harvest strain energy through deformation, the strategies of the mechanical structure optimization have rarely been reported.

Poisson's ratio is a fundamental mechanical property of materials, which relates the lateral strain to the applied strain. Materials with negative Poisson's ratio (NPR) exhibit auxetic behavior, i.e., the material would expand in the lateral direction when it is stretched under uniaxial tension. Piezoelectric devices with the NPR effect have been reported previously.^{34–36} In 1998, Baughman *et al.* mentioned that metals with the NPR effect may find application as electrodes that amplify the response of piezoelectric sensors.³⁴ For the case of piezoelectric energy harvesters, Li *et al.* performed finite element calculations and showed that the piezoelectric bimorph comprised an auxetic substrate sandwiched between two piezoelectric layers resulting in increased power output for vibration energy harvesting.³⁵ Ferguson *et al.* have demonstrated experimentally that piezoelectric vibration energy harvesters constructed with the auxetic substrate demonstrated enhanced electric power output.³⁶ These works indicate that the performance of piezoelectric energy harvesters can be effectively promoted by the NPR effect, but the incorporation of the NPR effect by using the auxetic steel substrates, to some extent, sacrifices the device flexibility. To utilize the effect of NPR in flexible piezoelectric energy harvesters, materials with both auxetic behavior and flexibility are required.

Graphene, the famous two-dimensional material of hexagonally arranged carbon sheet, has great potential in flexible electronics owing to its extraordinary properties.^{37,38} Applications of graphene and its derivative have also been demonstrated in piezoelectric energy harvesting.^{39–41} Very recently, our group has developed a graphene-assembled macro-film (GAMF), which possesses not only excellent flexibility and NPR but also high electrical conductivity.⁴² Owing to these extraordinary properties, the GAMF could be used as the electrodes to fabricate piezoelectric energy harvesters and thereby enhance the output performance by utilizing the NPR effect.

In this work, flexible piezoelectric energy harvesters with increased output performance are fabricated using GAMF electrodes. An analytical expression that describes the relationship between open-circuit voltage and Poisson's ratio of electrodes is theoretically derived. Further, experimental results on piezoelectric energy harvesters with GAMF electrodes are discussed and compared with the performances of the harvesters with silver electrodes. The results show that the open-circuit voltage and short-circuit current can be significantly increased by using the GAMF electrodes.

To illustrate the effect of Poisson's ratio on the electricity output performance, a tri-layer laminated structure model is considered, in which a piezoelectric layer is sandwiched between two electrode layers. Piezoelectric energy harvesters of this structure work in the d_{31} -mode by imparting uniaxial tension. Usually, the piezoelectric energy harvesters are fabricated with conventional electrodes having a positive Poisson's ratio [Fig. 1(a)]. The mechanical impact of these conventional electrodes on the piezoelectric material is thought to be minor and negligible, and the generated electricity is assumed to be exclusively contributed by the longitudinal strain S_1 . The reasons for the minor impact of conventional electrodes on the piezoelectric material are as follows:

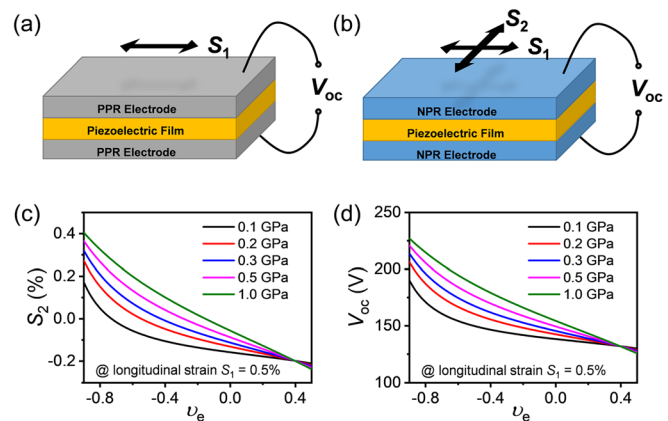


FIG. 1. Theoretical analysis of the effect of Poisson's ratio of the electrode on the electricity output performance. (a) Piezoelectric energy harvester using electrodes with a positive Poisson's ratio (PPR), in which the generated electricity is exclusively contributed by the longitudinal strain S_1 . (b) Piezoelectric energy harvester using electrodes with NPR, in which both of the longitudinal strain S_1 and the transverse strain S_2 have contributions to the generated electricity. (c) The transverse strain S_2 and (d) the open-circuit voltage V_{oc} as functions of Poisson's ratio ν_e of the electrode with various Young's modulus Y_e of the electrode.

(1) the conventional electrodes, such as conducting metal films and flexible plastics coated with conducting films,^{43,44} etc., have Poisson's ratios that are close to that of the piezoelectric layer, since both of them are positive; and (2) the electrodes are usually relatively thin, and, therefore, their tensile stiffness is much smaller than that of the piezoelectric material. In contrast, for the piezoelectric energy harvester with NPR electrodes [Fig. 1(b)], the mechanical impact of electrodes on the piezoelectric layer can be significant. It is expected that the entire harvester device would inherit auxetic behavior from the electrodes; thereby if the device is stretched in one direction (working in the d_{31} -mode), it will subsequently expand in the lateral direction (working in the d_{32} -mode) as well. In this way, both the longitudinal strain S_1 and the transverse strain S_2 contribute toward the conversion of mechanical energy into electricity, and, consequently, the electric output performance is enhanced.

To provide a more explicit demonstration of the above principle, expressions of the deformation and the open-circuit voltage of the tri-layer laminated structure model have been theoretically derived, starting from the elastic constitutive equation and piezoelectric equations. The following assumptions are applied: (1) under the condition that the in-plane dimensions are much larger than the thickness, the near-edge non-homogeneity of the electrical and mechanical quantities, including electric field, electric displacement, stress, strain, etc., are ignored, and all these quantities are assumed to be homogeneously distributed in each layer; (2) the mechanical coupling between the electrode and the piezoelectric layers is considered by assuming no relative sliding between the electrode and piezoelectric layers, i.e., the in-plane strains of different layers are the same; (3) the electrode material is isotropic, and the piezoelectric material is orthotropic; and (4) regarding the boundary conditions, the strain in the longitudinal direction S_1 is given and fixed, while all the other directions are stress-free.

According to the above assumptions, the transverse strain S_2 is expressed as

$$S_2 = \left(\frac{(v_p^D - v_e) \left(1 - (v_p^D)^2\right) t_e Y_e}{\left(1 - (v_p^D)^2\right) t_e Y_e + (1 - v_e^2) t_p Y_p^D} - v_p^D \right) S_1, \quad (1)$$

and the open-circuit voltage V_{oc} is expressed as

$$V_{oc} = \left(\frac{(v_p^D - v_e) \left(v_p^D g_{31} + g_{32}\right) t_e Y_e}{\left(1 - (v_p^D)^2\right) t_e Y_e + (1 - v_e^2) t_p Y_p^D} + g_{31} \right) \cdot t_p Y_p^D S_1, \quad (2)$$

where g_{31} and g_{32} are the piezoelectric voltage constants of the piezoelectric material; Y_p^D and v_p^D are the open-circuit Young's modulus and open-circuit Poisson's ratio of the piezoelectric material, respectively; Y_e and v_e are Young's modulus and Poisson's ratio of the electrode material, respectively; t_p is the thickness of the piezoelectric layer; and t_e is the total thickness of the upper and lower electrode layers ($t_e/2$ for each layer). Details of the derivation process are presented in the [supplementary material](#) (Sec. S1).

The transverse component of the strain, i.e., S_2 , and the open-circuit voltage V_{oc} as functions of Poisson's ratio v_e of the electrode with various Young's modulus Y_e are plotted in [Figs. 1\(c\)](#) and [1\(d\)](#), respectively, using the piezoelectric material parameters given in the [supplementary material](#) (Sec. S2). It can be seen that with the decrease in v_e , S_2 gradually increases, changing from negative (compressive strain) to positive (tensile strain). This indicates that the auxetic behavior of the electrodes renders the tri-layer laminated structure with auxetic behavior, which can be attributed to the mechanical coupling between the electrode and piezoelectric layers. As a result, V_{oc} also exhibits an increasing trend with the decrease in v_e , depicting the enhancement of output electricity using electrodes with NPR.

To utilize the NPR effect in flexible piezoelectric energy harvesters, the GAMF having excellent flexibility, high conductivity, and the NPR effect is developed. The GAMF was prepared from graphene oxide (GO, purchased from Wuxi Chengyi Education Technology Co. Ltd., China) via a process comprising dispersion in ultrapure water, formation of GO film by drying in glass mold, and finally reducing by high-temperature annealing (up to 3000 °C in an argon atmosphere). For the characterization of GAMF, Raman spectroscopy (LabRAM HR Evolution, HORIBA, Japan) and scanning electron microscopy (SEM, JSM-7610FPlus, JEOL, Japan) were employed. Before the observation of the cross sectional morphology, the GAMF specimen was fractured in liquid nitrogen. Poisson's ratio of GAMF was measured via non-contact method, using a full-field 3D strain measurement system (VIC-3D, Correlated Solution, America). Elaborate measurement of Poisson's ratio can be found in our previous paper.⁴²

[Figure 2\(a\)](#) shows that the GAMF possesses excellent flexibility, as it can be folded into an airplane. In addition, the conductivity of GAMF is very high (10^5 S/m).⁴² In the Raman spectrum of GAMF [[Fig. 2\(b\)](#)], G and 2D bands are located at 1582 cm^{-1} and 2722 cm^{-1} , respectively, whereas the D band is almost invisible, indicating that the GAMF is highly graphitized. The high degree of graphitization of

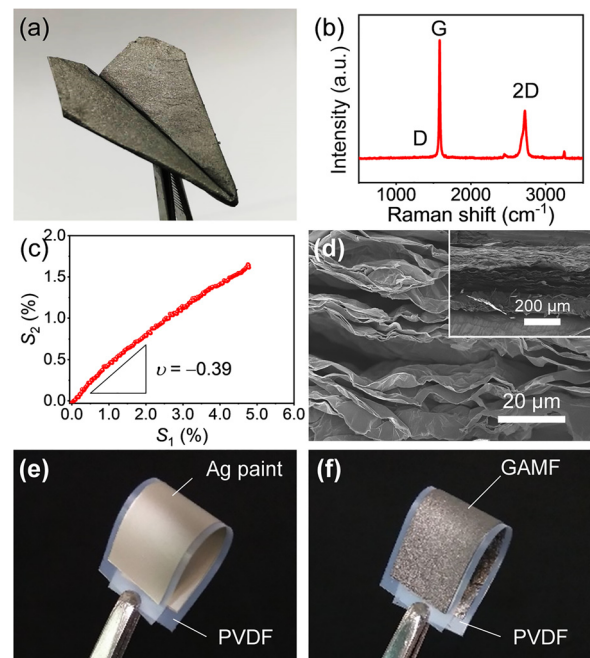


FIG. 2. Characterizations of the GAMF. (a) Photograph of a GAMF folded into an airplane. (b) Raman spectrum of GAMF. (c) The transverse strain S_2 vs longitudinal strain S_1 plot of GAMF under uniaxially tension. (d) Cross-sectional SEM images of GAMF. Photographs of (e) Ag/PVDF/Ag and (f) GAMF/PVDF/GAMF tri-layer laminated structures.

GAMF could be responsible for its high conductivity. [Figure 2\(c\)](#) shows that the GAMF has a negative Poisson's ratio of about -0.39 . The NPR of GAMF is associated with the presence of micro-wrinkles and pores,⁴² as shown by the cross-sectional SEM images in [Fig. 2\(d\)](#). The micro-wrinkles and pores are created by the high-temperature reducing process during the preparation of GAMF.⁴² [Figures 2\(e\)](#) and [2\(f\)](#) show the photographs of Ag/PVDF/Ag and GAMF/PVDF/GAMF tri-layer laminated structures, respectively. Because of the excellent flexibility of GAMF, the attachments of GAMF do not influence the flexibility of the PVDF film. Briefly, the excellent flexibility and conductivity equip the GAMF with the attributes to be used as electrodes in flexible electronic devices. Further, the NPR of GAMF also provides a golden opportunity to develop piezoelectric energy generator with high output performance.

We design a prototype flexible piezoelectric energy harvesting device, attempting to take advantages of the NPR effect of GAMF. [Figure 3\(a\)](#) schematically depicts the piezoelectric energy harvester device configuration. In the prototype device, the two ends of GAMF/PVDF/GAMF tri-layer laminated structure are fixed on a flexible polyethylene terephthalate (PET) substrate. The device is operated by bending the PET substrate [[Fig. 3\(b\)](#)], and in this manner, the GAMF/PVDF/GAMF tri-layer laminated structure is uniaxially stretched. The tensile strain in the GAMF/PVDF/GAMF tri-layer laminated structure is determined by the curvature of the PET substrate.

A commercial PVDF film (purchased from Jinzhoukexin Electronic Material Co. Ltd., China, and the electrodes for poling have been removed) with the thickness of $t_p = 50\text{ }\mu\text{m}$ and the piezoelectric

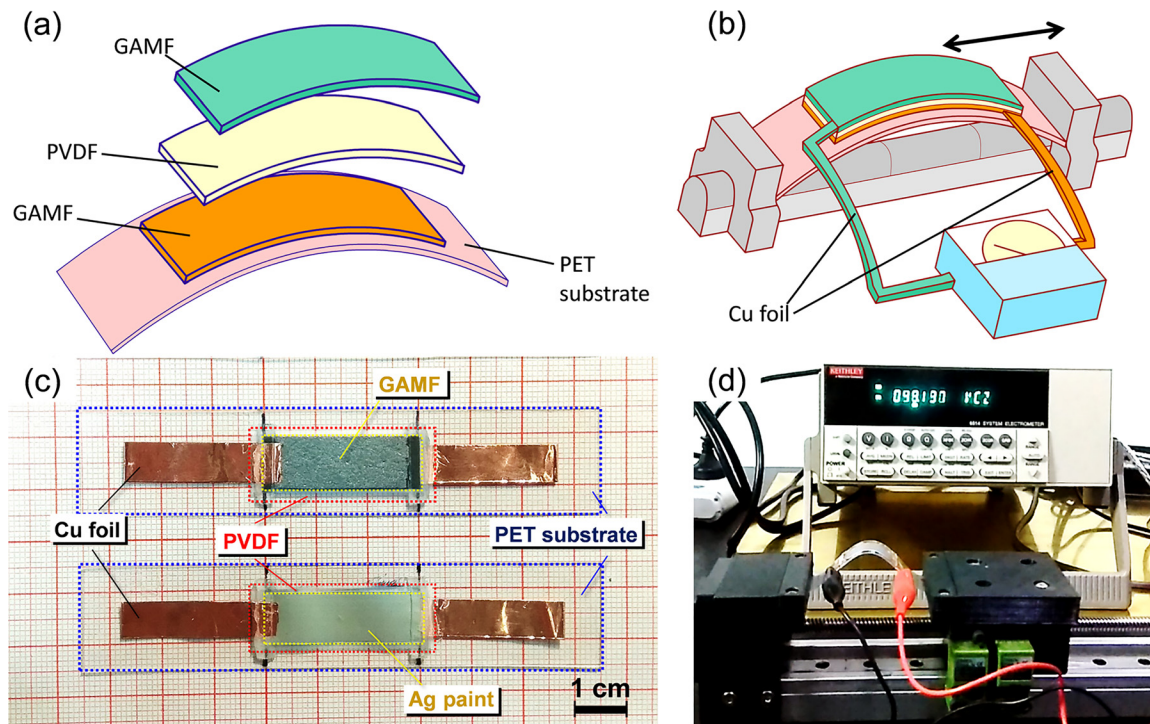


FIG. 3. Design and measurement of flexible piezoelectric energy harvester devices. Schematics of (a) the piezoelectric energy harvester device configuration and (b) the measurement setup of the electricity output performance. Photographs of (c) the fabricated devices and (d) the bending of the device during the measurement process.

strain constant of $|d_{33}| = 21$ pC/N was used in the device fabrication. Two pieces of the GAMF with the thickness of $200\ \mu\text{m}$ and the dimension of $3.0 \times 1.0\ \text{cm}^2$ were attached to the two opposite surfaces of a piece of PVDF film of area $3.5 \times 1.2\ \text{cm}^2$, respectively, using conductive silver paint (SPI Supplies, Structure Probe, Inc., America) to fabricate the GAMF/PVDF/GAMF tri-layer laminated structure. Subsequently, the two ends of the GAMF/PVDF/GAMF tri-layer laminated structure were fixed onto a flexible PET substrate with a lateral dimension of $10.0 \times 2.0\ \text{cm}^2$ and a thickness of $260\ \mu\text{m}$. For the purpose of comparison, the piezoelectric energy harvester devices constructed using silver electrodes have also been fabricated with the same design. Figure 3(c) shows the photograph of the devices. For the measurement of the output performance of the generated electricity, a customized bending machine was employed [Fig. 3(d)]. The harvester devices were operated in repeatedly bending with the open-circuit voltage and short-circuit current that were measured simultaneously by an electrometer (Keithley 6514, Keithley Instruments Inc., America). This process of measurement is also shown intuitively in the supplementary video (Video S1).

Figure 4(a) shows the typical waveforms of the open-circuit voltage and short-circuit current measured from the piezoelectric energy harvesters with GAMF and Ag electrodes. The frequency is about $0.76\ \text{Hz}$, which is determined by the bending machine. The electricity outputs in the forward and reverse connections confirm that the signals are generated from the piezoelectric effect. It is noted that the open-circuit voltage and short-circuit current of the piezoelectric energy harvesters with GAMF electrodes are

significantly higher than those of the devices with Ag electrodes. The comparative analysis of the peak-to-peak values of open-circuit voltage V_{pp} and short-circuit current I_{pp} is depicted in Fig. 4(b). For the piezoelectric energy harvesters with GAMF electrodes, $V_{pp} = (167.4 \pm 11.0)\ \text{V}$, $I_{pp} = (794.7 \pm 99.2)\ \text{nA}$ are recorded, and for the piezoelectric energy harvesters with Ag electrodes, $V_{pp} = (101.3 \pm 5.1)\ \text{V}$, $I_{pp} = (485.6 \pm 22.5)\ \text{nA}$ have been obtained. These data are the statistical results of four devices for each group, and each device has been measured for at least 100 s. A complete set of the measured results for each device is presented in Fig. 4(c). For each device, the electricity generation is a continuous process and is generally stable. Moreover, the open-circuit voltage and short-circuit current measured from each of the piezoelectric energy harvester devices constructed with GAMF electrodes are all greater than that of piezoelectric energy harvesters with Ag electrodes. These results demonstrate the advantages of the GAMF to be used as the electrodes in flexible piezoelectric energy harvesters and subsequently enhance their output performance.

To summarize, we have shown that the electricity output performance of flexible piezoelectric energy harvesters can be effectively enhanced by using the NPR electrodes. The GAMF, endowed with excellent flexibility, high conductivity, and the NPR effect, is used as the electrodes to fabricate prototype flexible piezoelectric energy harvester. The harvesters with GAMF electrodes exhibit significantly enhanced open-circuit voltage and short-circuit current compared with the harvesters constructed with silver electrodes in the same

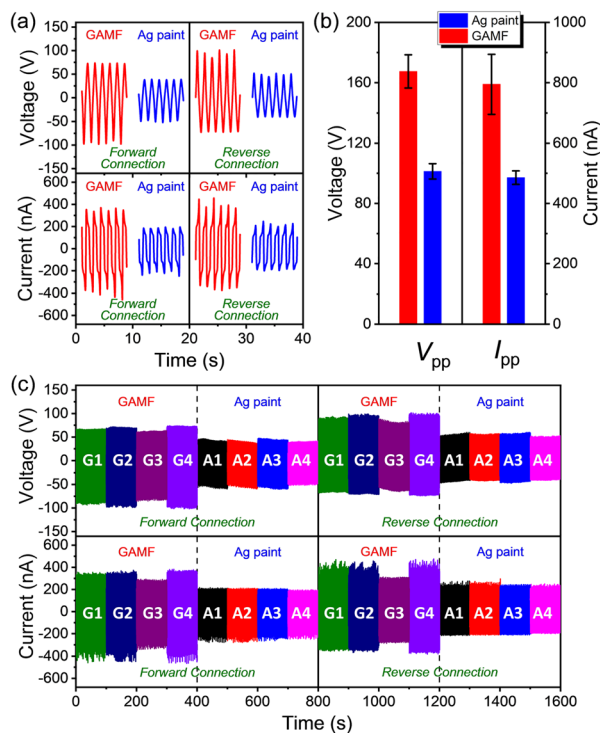


FIG. 4. Comparisons of the electricity output performance of flexible piezoelectric energy harvester devices with GAMF and Ag electrodes. (a) Typical waveforms of the open-circuit voltage and short-circuit current. (b) Statistical results of the peak-to-peak values of open-circuit voltage V_{pp} and short-circuit current I_{pp} . (c) Complete set of the measured results of four devices for each group.

design. These results indicate that the GAMF has potential applications in flexible piezoelectric energy harvesters.

See the [supplementary material](#) for the details of theoretical derivation, the material parameters in plotting [Figs. 1\(c\)](#) and [1\(d\)](#), and a video of the electrical measurement of the devices.

AUTHORS' CONTRIBUTIONS

H.Z. and P.W. contributed equally to this work.

This work was financially supported by the National Natural Science Foundation of China (Nos. 51701146 and 11902232), the Equipment Pre-Research Joint Fund of EDD and MOE (No. 6141A02022262), the Post-Doctoral Innovation Research Project of Hubei Province (No. 20201jb003), and the Fundamental Research Funds for the Central Universities (WUT: Nos. 2018III019 and 2019IVA108).

DATA AVAILABILITY

The data that support the findings of this study are available from the corresponding author upon reasonable request.

REFERENCES

¹J. H. Park, H. E. Lee, C. K. Jeong, D. H. Kim, S. K. Hong, K.-I. Park, and K. J. Lee, *Nano Energy* **56**, 531–546 (2019).

- ²F. Yi, H. Ren, J. Shan, X. Sun, D. Wei, and Z. Liu, *Chem. Soc. Rev.* **47**, 3152–3188 (2018).
- ³X. Mo, H. Zhou, W. Li, Z. Xu, J. Duan, L. Huang, B. Hu, and J. Zhou, *Nano Energy* **65**, 104033 (2019).
- ⁴B. Li, F. Zhang, S. Guan, J. Zheng, and C. Xu, *J. Mater. Chem. C* **4**, 6988–6995 (2016).
- ⁵D. Yao, H. Cui, R. Hensleigh, P. Smith, S. Alford, D. Bernero, S. Bush, K. Mann, H. F. Wu, M. Chin-Nieh, G. Youmans, and X. Zheng, *Adv. Funct. Mater.* **29**, 1903866 (2019).
- ⁶N. A. Shepelin, A. M. Glushenkov, V. C. Lussini, P. J. Fox, G. W. Dicinowski, J. G. Shapter, and A. V. Ellis, *Energy Environ. Sci.* **12**, 1143–1176 (2019).
- ⁷S. S. Won, M. Kawahara, C. W. Ahn, J. Lee, J. Lee, C. K. Jeong, A. I. Kingon, and S.-H. Kim, *Adv. Electron. Mater.* **6**, 1900950 (2020).
- ⁸Y. Zhang, C. K. Jeong, T. Yang, H. Sun, L.-Q. Chen, S. Zhang, W. Chen, and Q. Wang, *J. Mater. Chem. A* **6**, 14546–14552 (2018).
- ⁹J. Yan, M. Liu, Y. G. Jeong, W. Kang, L. Li, Y. Zhao, N. Deng, B. Cheng, and G. Yang, *Nano Energy* **56**, 662–692 (2019).
- ¹⁰M. B. Khan, D. H. Kim, J. H. Han, H. Saif, H. Lee, Y. Lee, M. Kim, E. Jang, S. K. Hong, D. J. Joe, T.-I. Lee, T.-S. Kim, K. J. Lee, and Y. Lee, *Nano Energy* **58**, 211–219 (2019).
- ¹¹W. S. Jung, M. G. Kang, H. G. Moon, S. H. Baek, S. J. Yoon, Z. L. Wang, S. W. Kim, and C. Y. Kang, *Sci. Rep.* **5**, 9309 (2015).
- ¹²W. Wang, J. Zhang, Y. Zhang, F. Chen, H. Wang, M. Wu, H. Li, Q. Zhu, H. Zheng, and R. Zhang, *Appl. Phys. Lett.* **116**, 023901 (2020).
- ¹³J. Gui, Y. Zhu, L. Zhang, X. Shu, W. Liu, S. Guo, and X. Zhao, *Appl. Phys. Lett.* **112**, 072902 (2018).
- ¹⁴D. Hu, M. Yao, Y. Fan, C. Ma, M. Fan, and M. Liu, *Nano Energy* **55**, 288–304 (2019).
- ¹⁵Z. L. Wang and J. Song, *Science* **312**, 242 (2006).
- ¹⁶R. Yang, Y. Qin, L. Dai, and Z. L. Wang, *Nat. Nanotechnol.* **4**, 34–39 (2009).
- ¹⁷W. Wu, L. Wang, Y. Li, F. Zhang, L. Lin, S. Niu, D. Chenet, X. Zhang, Y. Hao, T. F. Heinz, J. Hone, and Z. L. Wang, *Nature* **514**, 470 (2014).
- ¹⁸G.-J. Lee, M.-K. Lee, J.-J. Park, D. Y. Hyeon, C. K. Jeong, and K.-I. Park, *ACS Appl. Mater. Interfaces* **11**, 37920–37926 (2019).
- ¹⁹C. Chang, V. H. Tran, J. Wang, Y.-K. Fuh, and L. Lin, *Nano Lett.* **10**, 726–731 (2010).
- ²⁰N. Soin, T. H. Shah, S. C. Anand, J. Geng, W. Pornwannachai, P. Mandal, D. Reid, S. Sharma, R. L. Hadimani, D. V. Bayramol, and E. Siores, *Energy Environ. Sci.* **7**, 1670–1679 (2014).
- ²¹X. Chen, H. Tian, X. Li, J. Shao, Y. Ding, N. An, and Y. Zhou, *Nanoscale* **7**, 11536–11544 (2015).
- ²²K.-I. Park, J. H. Son, G.-T. Hwang, C. K. Jeong, J. Ryu, M. Koo, I. Choi, S. H. Lee, M. Byun, Z. L. Wang, and K. J. Lee, *Adv. Mater.* **26**, 2514–2520 (2014).
- ²³G.-T. Hwang, V. Annapureddy, J. H. Han, D. J. Joe, C. Baek, D. Y. Park, D. H. Kim, J. H. Park, C. K. Jeong, K.-I. Park, J.-J. Choi, D. K. Kim, J. Ryu, and K. J. Lee, *Adv. Energy Mater.* **6**, 1600237 (2016).
- ²⁴C. K. Jeong, K.-I. Park, J. H. Son, G.-T. Hwang, S. H. Lee, D. Y. Park, H. E. Lee, H. K. Lee, M. Byun, and K. J. Lee, *Energy Environ. Sci.* **7**, 4035–4043 (2014).
- ²⁵G.-T. Hwang, H. Park, J.-H. Lee, S. Oh, K.-I. Park, M. Byun, H. Park, G. Ahn, C. K. Jeong, K. No, H. Kwon, S.-G. Lee, B. Joung, and K. J. Lee, *Adv. Mater.* **26**, 4880–4887 (2014).
- ²⁶G.-T. Hwang, J. Yang, S. H. Yang, H.-Y. Lee, M. Lee, D. Y. Park, J. H. Han, S. J. Lee, C. K. Jeong, J. Kim, K.-I. Park, and K. J. Lee, *Adv. Energy Mater.* **5**, 1500051 (2015).
- ²⁷J. Kwon, W. Seung, B. K. Sharma, S.-W. Kim, and J.-H. Ahn, *Energy Environ. Sci.* **5**, 8970–8975 (2012).
- ²⁸K.-I. Park, M. Lee, Y. Liu, S. Moon, G.-T. Hwang, G. Zhu, J. E. Kim, S. O. Kim, D. K. Kim, Z. L. Wang, and K. J. Lee, *Adv. Mater.* **24**, 2999–3004 (2012).
- ²⁹C. K. Jeong, K.-I. Park, J. Ryu, G.-T. Hwang, and K. J. Lee, *Adv. Funct. Mater.* **24**, 2620–2629 (2014).
- ³⁰K.-I. Park, C. K. Jeong, J. Ryu, G.-T. Hwang, and K. J. Lee, *Adv. Energy Mater.* **3**, 1539–1544 (2013).
- ³¹G. Zhang, P. Zhao, X. Zhang, K. Han, T. Zhao, Y. Zhang, C. K. Jeong, S. Jiang, S. Zhang, and Q. Wang, *Energy Environ. Sci.* **11**, 2046–2056 (2018).
- ³²H. Liu, J. Zhong, C. Lee, S. W. Lee, and L. Lin, *Appl. Phys. Rev.* **5**, 041306 (2018).
- ³³Z. Yang, S. Zhou, J. Zu, and D. Inman, *Joule* **2**, 642–697 (2018).

- ³⁴R. H. Baughman, J. M. Shacklette, A. A. Zakhidov, and S. Stafström, *Nature* **392**, 362–365 (1998).
- ³⁵Q. Li, Y. Kuang, and M. Zhu, *RSC Adv.* **7**, 015104 (2017).
- ³⁶W. J. G. Ferguson, Y. Kuang, K. E. Evans, C. W. Smith, and M. Zhu, *Sens. Actuators, A* **282**, 90–96 (2018).
- ³⁷R. Ma, Y. Zhou, H. Bi, M. Yang, J. Wang, Q. Liu, and F. Huang, *Prog. Mater. Sci.* **113**, 100665 (2020).
- ³⁸S. K. Reddy and A. Ya'akovovitz, *Appl. Phys. Lett.* **115**, 211902 (2019).
- ³⁹M. Ye, Z. Zhang, Y. Zhao, and L. Qu, *Joule* **2**, 245–268 (2018).
- ⁴⁰R. A. Surmenev, T. Orlova, R. V. Chernozem, A. A. Ivanova, A. Bartasyte, S. Mathur, and M. A. Surmenev, *Nano Energy* **62**, 475–605 (2019).
- ⁴¹D. K. Bharti, M. K. Gupta, R. Kumar, N. Sathish, and A. K. Srivastava, *Nano Energy* **73**, 104821 (2020).
- ⁴²P. Li, Z. Wang, R. Song, W. Qian, P. Wen, Z. Yang, and D. He, *Carbon* **162**, 545–551 (2020).
- ⁴³Y. Zhang, W. Zhu, C. K. Jeong, H. Sun, G. Yang, W. Chen, and Q. Wang, *RSC Adv.* **7**, 32502–32507 (2017).
- ⁴⁴Y. Zhang, M. Wu, Q. Zhu, F. Wang, H. Su, H. Li, C. Diao, H. Zheng, Y. Wu, and Z. L. Wang, *Adv. Funct. Mater.* **29**, 1904259 (2019).